ACCEPTED VERSION

Hartnett, John; Tobar, Michael; Ivanov, Eugene; Luiten, André N. ,
Optimum design of a high-Q room-temperature Whispering-Gallery-mode x-band sapphire resonator,
IEEE Transactions on Ultrasonics, Ferroelectrics and Frequency Control, 2013; InPress

http://hdl.handle.net/2440/77266

Optimum Design of a High-Q Room-Temperature Whispering-Gallery-Mode X-band Sapphire Resonator

John G. Hartnett[1,2], Michael E. Tobar[1], Fellow of
IEEE, Eugene N. Ivanov[1] and Andre N. Luiten[1,2*]

[1]*School of Physics, University of Western Australia*

35 Stirling Hwy Crawley 6009 W.A. Australia

[2]*IPAS, School of Chemistry and Physics,*

University of Adelaide, Adelaide, 5005 S.A. Australia

(Dated: April 15, 2013)

Abstract

A process for optimal design of a room temperature Whispering Gallery mode sapphire resonator has been developed. In particular, design rules were determined to enable choice of the optimum azimuthal mode number and resonator radius for a given resonance frequency. The coupling probe design was investigated and it was found that straight antenna probes aligned radially and positioned in the mid-plane of the resonator gave the highest unloaded Q-factors due to minimized probe losses. We noted that when coupling through this technique (as compared with a perpendicular-positioned probe) the mode standing wave pattern would lock to some asymmetry in the crystal resonator itself and not to the probe. This was confirmed by noting that the coupling could be altered over a significant range by mere rotation of the resonator. Following these optimal design rules we were able to measure the Q-factors of quasi-TE and quasi-TM modes with high precision in four cylindrical sapphire resonators at room temperature. The highest attainable Q-factor was $(2.1 \pm 0.1) \times 10^5$ at 9 GHz in a quasi-TM mode.

Keywords: sapphire resonator, Q-factor, Whispering Gallery modes, coupling probes

---

*Electronic address: `john.hartnett@adelaide.edu.au`

I.   INTRODUCTION

Low phase noise oscillators are crucial for modern radar and telecommunication systems. Extremely low phase noise of the order of -160 dBc/Hz in the microwave regime at Fourier frequencies near 1 kHz has been demonstrated by [1, 2] with advanced phase noise reduction techniques using interferometric carrier suppression. The high quality-factor of Whispering Gallery (WG) sapphire resonators ($Q > 10^5$ at room temperature) was the essential element of this achievement. Nonetheless, at low Fourier frequencies (below 1 Hz), the best quartz oscillators still demonstrate superior phase noise performance over the sapphire devices [3, 4].

In contrast, at cryogenic temperatures the sapphire devices can show extremely high Q-factors together with low frequency-temperature coefficients, and thus it is possible to obtain much improved phase noise at these low Fourier frequencies ($\sim 1\,\mathrm{Hz}$ offset from the carrier) [5, 6]. Nonetheless, the simplicity of the room temperature oscillators demands that one consider whether it is possible to improve the close-in-to-the-carrier phase noise by optimizing the quality-factor of the dielectric resonator [7–12]. The highest Q-factor yet reported in a sapphire dielectric resonator near room temperature ($269\,\mathrm{K}$) was 2.3×10^5 [3, 13] and in this paper, we report on the processes necessary to achieve this performance.

II.   SAPPHIRE RESONATORS

The microwave losses in four different cylindrical sapphire samples were measured using the Whispering Gallery mode method [14, 15] and the loss tangent results reported [16]. Two of the resonators were manufactured by Crystal Systems (CS) with dimensions 24×22 (diameter [mm] × height [mm] respectively) and $50 \times 20 - 24$. The latter had a tapered height ranging from 24.50 mm in the center down to 20.27 mm at the diameter. One resonator was manufactured by Union Carbide (UC) with dimensions 45×30 and the fourth was Russian grown with dimensions 40×20. We measured the properties of the fundamental $WGH_{m,0,0}$ mode and $WGE_{m,0,0}$ mode families in all four resonators at room temperature. In the Russian grown sapphire the $WGH_{m,0,0}$ mode family was also measured at 274 K. In addition the $WGH_{9,0,0}$ and the $WGE_{7,0,0}$ modes were measured as a function of temperature.

The resonators losses, coupling and mode frequency were analyzed in reflection with a coupling factor set to be significantly less than 1. The measurement setup is shown
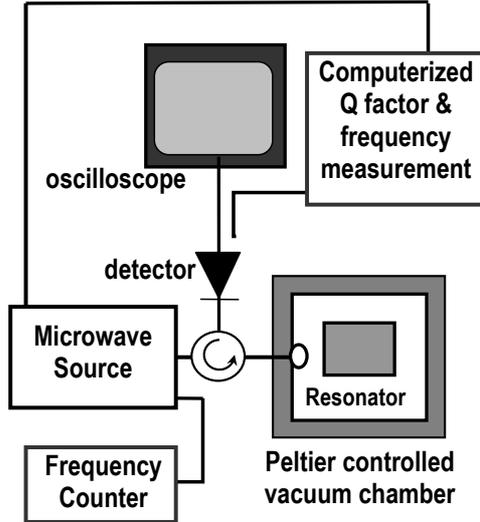
2

FIG. 1: The measurement setup, shown here for measurement of resonance modes in reflection using a loop probe through the side shield. Straight antenna probes were also used from the side as well as through the top shield.

in Fig. 1. A stable swept microwave probe signal was created by mixing the output of an HP 8673G synthesizer with a Marconi 2030 synthesizer (Microwave source in Fig 1). Custom designed software controlled the sweep and fitted a Lorentzian to the resonance line shape of the reflected signal [17] to produce an automated measurement procedure. The resonance frequencies were determined by the frequency at minimum reflection, and the loaded Q-factor was calculated from the bandwidth determined by the Lorentzian fit. Once the resonator reached temperature equilibrium, the program was left to repetitively measure the frequency, Q-factor and coupling. All synthesizers were phase-locked to an external high-stability reference source. The coupling (β) was determined from,

$$\beta = \frac{1 - \sqrt{P_{on}/P_{off}}}{1 + \sqrt{P_{on}/P_{off}}}, \tag{1}$$

provided undercoupled. Here P_{on} and P_{off} represent the power on and off resonance, respectively, which were determined with a tunnel diode detector operating in a low power regime, well below saturation.

In the case where temperature control was necessary, the resonator was housed in a vacuum chamber thermally contacted to a thermoelectric (Peltier) module. One side of Peltier element was contacted to the cavity, while the other was heat sunk to the outside. The temperature was measured using a lock-in amplifier to sense the imbalance signal from
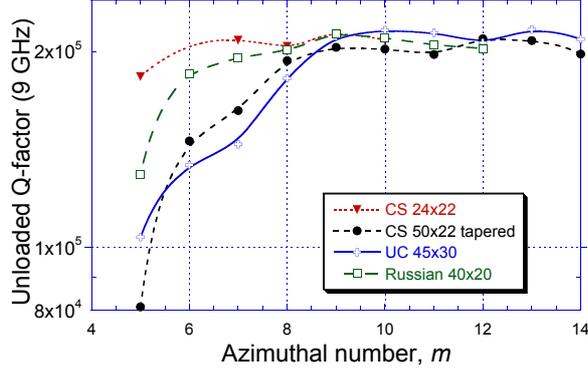
FIG. 2: The unloaded Q-factor of the $WGH_{m,0,0}$ mode measured in 4 different sapphire samples at 296 K, normalized to a frequency of 9 GHz for each mode of azimuthal mode number, m, according to Eq. (1). The smooth fitted lines are a guide to the eye only.
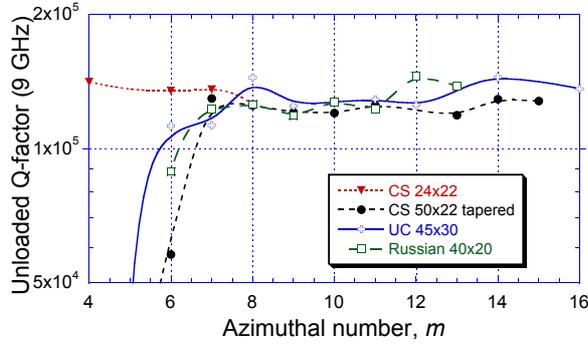

FIG. 3: The unloaded Q-factor of the $WGE_{m,0,0}$ mode measured in 4 different sapphire samples at 296 K, normalized to a frequency of 9 GHz for each mode of azimuthal mode number, m, according to Eq. (1). The smooth fitted lines are a guide to the eye only.

a custom-designed ac-bridge which used a thermistor in one arm. The output of the locking amplifier was sent to a PID controller and then onto a thermoelectric element. The desired temperature was set by a variable resistor in the ac-bridge. When the set point was varied the resonator was allowed to come to equilibrium before the frequency, Q-factor, coupling and temperature were measured. Any thermal gradients were monitored and determined using a calibrated thermistor connected to the opposite side of the cavity from the Peltier and control thermistor.

III. Q-FACTOR OF SAPPHIRE

The unloaded quality factor was measured at room temperature for each mode in the whispering gallery $WGH_{m,0,0}$ (quasi-TM) and $WGE_{m,0,0}$ (quasi-TE) mode families. This data is displayed on Figs 2 and 3 respectively where we have normalized to 9 GHz according to the following,

$$Q(9 \text{ GHz}) = Q_0 \times \frac{f_0}{9}, \tag{2}$$

where Q_0 and f_0 are, respectively, the unloaded Q-factor and the frequency (in GHz) of the measured resonance mode.

This normalization is equivalent to keeping the aspect ratio of the resonator constant and varying the diameter until the frequency of the chosen mode with a given azimuthal number (m) is 9 GHz. From this it was determined that the maximum Q-factor attainable in sapphire at 9 GHz and 296 K in a $WGH_{m,0,0}$ mode is $(2.1 \pm 0.1) \times 10^5$ and in a $WGE_{m,0,0}$ mode is $(1.3 \pm 0.1) \times 10^5$, which is set by the respective dielectric losses parallel and perpendicular to the crystal axis [14–16].

The normalization shown in Figs 2 and 3 help us see when the optimal Q-factor is reached as a function of azimuthal mode number (m) for a chosen mode frequency (f_0). This occurs when a maximum value is reached. This is equivalent to the $Q_0 \times f_0$ product becoming a constant and therefore the unloaded Q-factor of the resonator becomes inversely proportional to mode frequency and is limited predominantly by dielectric losses.

The additional losses seen in Figs 2 and 3 for low azimuthal mode numbers are the result of the quality factor being partially limited by shield losses. At $m \leq 6$ shield surface resistance becomes particularly important. In one resonator the Q-factor was measured to be 1.9×10^5 with a polished silver-plated shield while after some time exposed to the environment in the lab, and the silver tarnishes in air affecting the surface resistivity of the shield, the measured Q-factor degraded to 6.6×10^4. Only at sufficiently high values of the azimuthal mode index m do wall losses become insignificant allowing the Q-factor to be limited by pure dielectric losses. The errors we have quoted in the maximal Q-factors are derived from the scatter between results obtained in the different resonators. The measurements themselves have a random error of around 10%, which was determined by comparison between our technique and the results derived from a vector network analyzer when the cavity was extremely under-coupled.
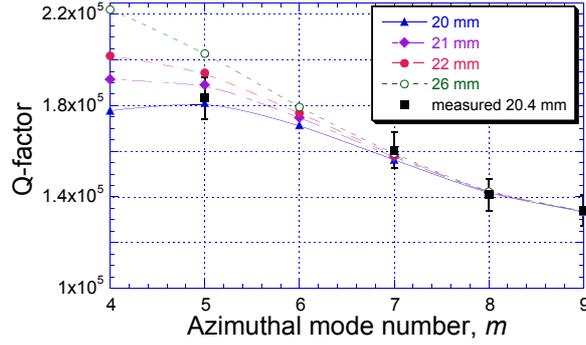
FIG. 4: A family of curves predicting the Q-factor of the $WGH_{m,0,0}$ mode family in the $24 \times 22\,\mathrm{mm}$ shielded sapphire resonator as a function of shield radius. Also shown is the measurements we have made on the 20.4mm diameter resonator. The smooth fitted lines are a guide to the eye only.
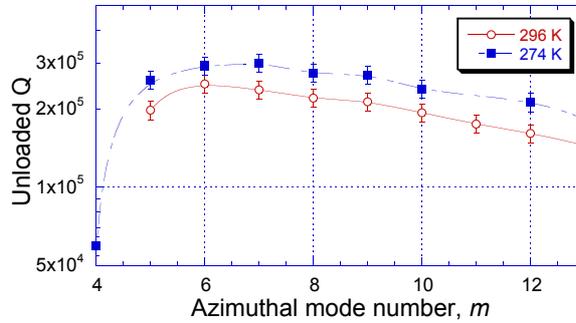

FIG. 5: The Q-factor of the $WGH_{m,0,0}$ mode family in the Russian-grown $40 \times 20\,\mathrm{mm}$ shielded sapphire resonator at both 296 K and 274 K. The smooth fitted lines are a guide to the eye only.

IV.   OPTIMUM AZIMUTHAL MODE NUMBER

Using the experimentally determined loss tangent values measured at 296 K, finite element calculations were used to predict the Q-factor of a shielded sapphire resonator with dimension $24 \times 22\,\mathrm{mm}$ as a function of shield radius. Figure 4 shows these predictions along with a set of measurements which are in close agreement with the modeling. The solid square data are the measured Q values for the $WGH_{m,0,0}$ mode family measured in the 24×22 resonator, which had a shield radius of 20.4 mm. For $m \geq 7$ the effects of the wall losses are clearly negligible at 296 K as the resulting Q-factor becomes independent of the resonator diameter. The decreasing Q factor at higher mode-numbers is associated with the increase in the loss tangent as the frequency increases [16].

The Q-factors of the $WGH_{m,0,0}$ mode family were compared at two different temperatures,

6

296 K and 274 K in the Russian grown 40×20 resonator (see Fig. 5). At 274 K the maximum Q-factor of $(3.0 \pm 0.2) \times 10^5$ occurs at $m = 7$ and 7.44 GHz. At 9.00 GHz with $m = 9$ the Q-factor was measured to be $(2.7 \pm 0.2) \times 10^5$, which is 17% higher than cited in [13].

V. DESIGN RULE

In order to facilitate construction of an optimized resonator we have developed a number of design rules. First one should choose an operational frequency which determines the resonator size given a minimum azimuthal mode number. If one also has constraints on shield size then it is possible to predict the maximum Q-factor before construction.

Figure 6 shows the linear relationship between the resonator's diameter and the azimuthal mode number at constant frequency, where we have chosen 9 GHz as the desired frequency. The slight deviations from the line are the result of the different aspect radios of the four resonators measured. If one chooses a sufficiently high mode number then the Q-factor will not be dependent on wall losses, which in turn means that the mode frequency will be minimally dependent on the position and surface reactance of the shield. One predicts that the resonator will thus be less sensitive to external vibrations, which can modulate the spacing between the resonator and the shield and probe. In this case, $m = 8$ means the diameter of the resonator should be 35 mm (indicated by broken lines in Fig. 6). Choosing a higher mode-number results in a larger resonator which will be more prone to vibration and cost more without any net benefit to the Q-factor. If one wishes to design a resonator with a different mode-frequency then it is possible to linearly scale the curve shown in Fig. 6 i.e. for a 4.5 GHz mode with $m = 8$ the diameter of the resonator should be 70 mm.

Figure 7 shows the linear dependence for optimum Q-factor on a resonator's diameter at constant frequency using the same measured data at 9 GHz. Provided the resonator shield radius is sufficiently optimized, the Q-factor may be read off as a function of resonator diameter. Optimized here means that the shield radius is optimally chosen as illustrated in Fig. 4. For the chosen azimuthal mode number the shield radius is sufficiently large enough such that contributions from the shield (wall losses) are minimized. This means the Q-factor $Q_s = G/R_s$ due to the shield is large because the Geometric factor (G) is large. Here R_s

represents the surface resistivity of the shield. The measured Q-factor is related by,

$$\frac{1}{Q_0} = p_{\epsilon\parallel} tan\delta_{d\parallel} + p_{\epsilon\perp} tan\delta_{d\perp} + \frac{R_s}{G}, \tag{3}$$

where p_ϵ represents the electric energy filling factors parallel and perpendicular to the crystal/cylinder axis. And $tan\delta_d$ represent the parallel and perpendicular components of the dielectric loss tangent for the sapphire crystal. For whispering gallery modes p_ϵ can be assumed equal to either 1 or 0 depending on the dominant polarization parallel or perpendicular to the cylinder axis [14, 15]. If either G is too small or R_s is too large the third term in Eq. (3) will dominate over the first two.

The measured data point at diameter of 24 mm indicates a low Q-factor due to a contribution from wall losses, which we can reduce by increasing the shield radius (to at least 26 mm for the WGH mode at 9 GHz with $m = 5$ as shown in Fig. 4), and hence increasing G, as indicated by the open circle in Fig. 7. However, for $m > 7$ as long as the shield radius is larger than 20 mm then the shield has negligible effect on the Q-factor. For example, at a diameter of 35 mm ($m = 8$) from Fig. 7 we predict a Q = 2.17×10^5 at 296 K. This Q-factor can be increased even further by cooling the resonator with a thermoelectric cooler. This means the dielectric losses in Eq. (3) are decreased. Based on the temperature dependence of the loss tangent [16] we predict this mode will have a Q-factor of 3×10^5 at 264 K. This is confirmed by the measurements of the Russian grown crystal at two different temperatures. In Fig. 5 we see that for $m > 7$ the unloaded Q as a function of azimuthal mode number m is only limited by the dielectric losses in the material and hence not limited by the shield losses.

VI. COUPLING PROBES

We investigated microwave coupling to the resonator using both top and side mounted probes (Figure 8). In the past it was found that the probe position could be a critical feature in determining the azimuthal location of the field anti-nodes in the standing wave microwave mode. Certainly this has been our experience with constructing cryogenic resonators [19]. In circumstances where the field probe was sufficiently weakly coupled to the resonator it is possible for the mode field to lock itself to some imperfection in the resonator crystal which break the cylindrical symmetry (i.e. a tilt of the crystal axis or a manufacturing flaw).
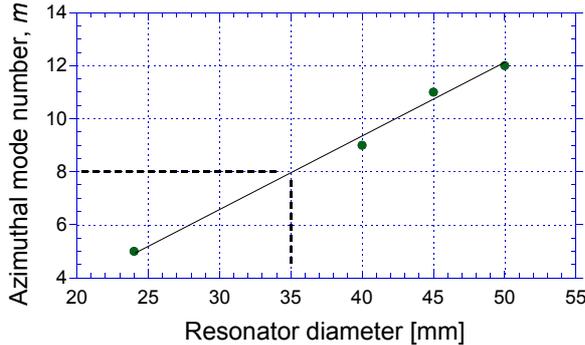
FIG. 6: A resonator's diameter as a function of the azimuthal mode number (m) at constant frequency. The highest Q-factor mode family in sapphire, $WGH_{m,0,0}$ modes, at 9 GHz was measured in the 4 different resonators.
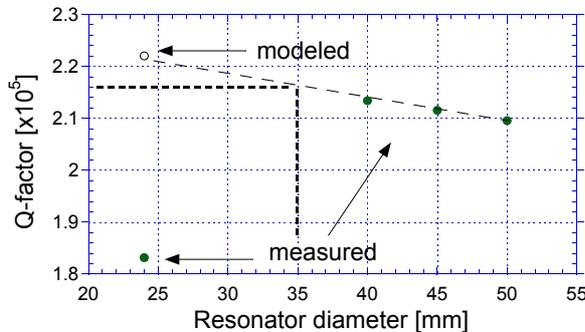

FIG. 7: Measured Q-factor as a function of resonator diameter (solid (green) circles). The modeled value (open circle) is shown for the Q-factor when the wall radius is sufficiently optimized. The broken line indicates a linear dependence, for optimum Q-factor, on the resonator diameter at constant frequency.

Thus the azimuthal "petal" pattern of field maxima and minima are not determined by the position of the probe but by some feature in the crystal.

We measured the highest unloaded Q-factor in a WGH-mode by coupling through the top of the cavity using a straight electric-field antenna probe parallel to the cylinder axis (E_z probe) to the dominant electric field component (top in Fig. 8). This method introduced less probe losses than coupling with an antenna probe from the side (E_r probe) to the electric-field component in the azimuthal (ϕ) direction, which is very weak in a WGH-mode (side ports 1 and 2 in Fig. 8). We also tried to couple to the resonator using a magnetic-field sensitive loop probe in the medial plane of the resonator (from the side, see Fig. 1) to couple to the azimuthal magnetic-field component and noted that this was also 10% below
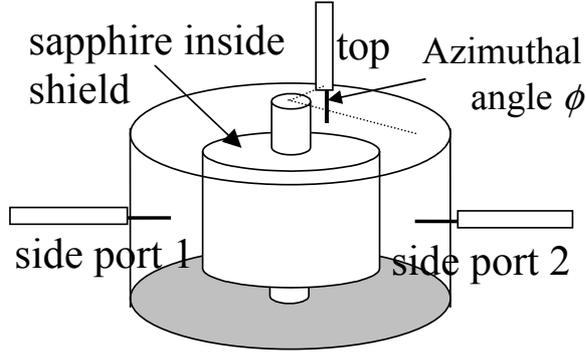
FIG. 8: Coupling probes were positioned as shown. The two side ports were at an azimuthal angle $\phi = 0$ and 180 degs, while the top port was at 90 degs.

the Q-factor measured using the top mounted electric field probe. When examining coupling to a WGE-mode we found optimal coupling, and minimal probe losses when using a straight antenna probe that coupled to the E_r field in the median plane of the resonator (side port 1 or 2 in Fig. 8).

When coupling to a WGH-mode through only the E_z probe from the top it was possible to observe that the coupling was periodically modulated between a very small value and some maximum value as a function of the azimuthal angle of the probe (ϕ on Fig. 8). This indicates that the electromagnetic standing wave pattern is locked to some feature of the crystal and not to the excitation probe. When at least one E_r probe was introduced in the medial plane it was observed that the field pattern locked to the position of that probe. In fact, for the WGH-mode when the E_r probe is positioned at the azimuthal angle (ϕ) of 90° with respect to the E_z probe, then one notes that the E_z probe is at a node in the field for an even mode-number mode.

On Fig. 9 we demonstrate the effect of this observation. We show the coupling of the WGH-mode family to the E_z probe. The coupling to this WGH family through a side port E_r probe (set so that it has unity coupling for the WGE-mode family) was about 25 dB less [18]. Nonetheless, it was observed that the presence of this weakly coupled side probes presence was sufficient to determine the azimuthal location of the mode-field maxima. We see that the even-numbered m modes have a small coupling because the E_r probe has forced a node at its location which consequently sets a node at the top coupling port positioned 90° degs around the circumference. In the case of odd-numbered m modes, we note that there must be a field anti-node at the location of the top coupling port which is evidenced
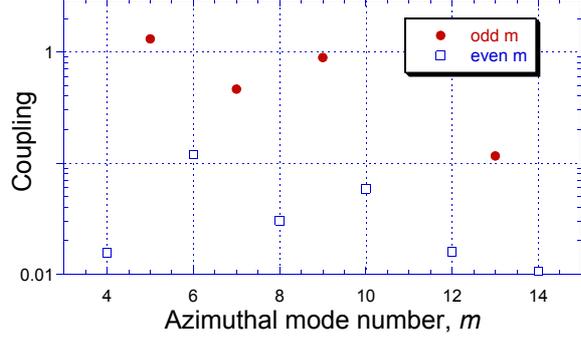
10

FIG. 9: The resonator coupling measured in reflection from the top with the parallel-positioned probe for the family of $WGH_{m,0,0}$ modes at 274 K. Coupling for odd numbered m are solid (red) circles and the even numbered m are open (blue) circles.
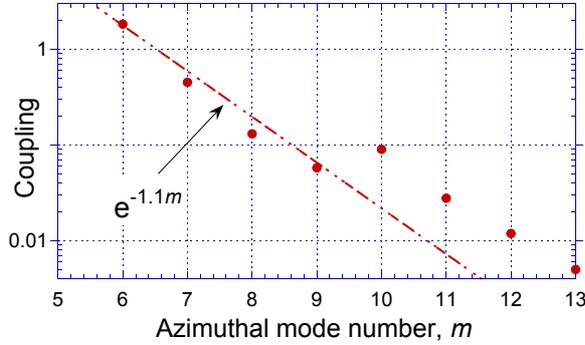

FIG. 10: The resonator coupling measured in reflection from the side port with the perpendicular-positioned probe for the family of $WGE_{m,0,0}$ modes at 296 K. The antenna probe in this case is parallel to the dominant electric field component perpendicular to the crystal axis.

by the fact that the coupling to these modes is much higher. We note that the coupling falls off for higher mode-numbers because the scale length of the evanescent field is shorter for these more confined modes.

When coupling to the $WGE_{m,0,0}$ mode family with a radial electric -field probe in the medial plane (i.e. coupled to the E_r component) it was observed that the electromagnetic mode was positioned so that there was a field maxima at the position of the exciting probe. Figure 10 shows that the coupling on this port reduces as a function of m (or frequency f) due to the higher confinement of the field for higher mode numbers. We can obtain a scale length for the field defined as $-\ln(\beta)/m$, which for this $WGE_{m,0,0}$ mode data, evaluates as either 1.1 ($m \leq 9$) or 1.0 ($m \geq 10$). The exponential fall off arises because the evanescent field
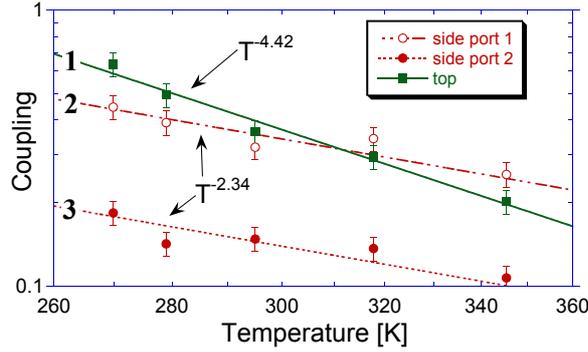
11

FIG. 11: The coupling to the $WGH_{9,0,0}$ (8.91 GHz) mode (curve 1) and to the $WGE_{7,0,0}$ (8.99 GHz) mode (curves 2 and 3) in the Russian grown 40×20 resonator measured as a function of temperature between 270 K and 350 K. The power law temperature dependence are shown for side and top coupling ports.

has an exponential dependence on the distance of the probe from the resonator normalized to the appropriate scale length of the mode. In this case, since the probe distance is fixed for all modes it leads to an exponential dependence on the scale length itself. The cause of the offset between $m = 9$ and 10 was not determined but is potentially associated with a movement of the field maxima for these higher frequency modes.

The coupling on the side ports to the $WGE_{7,0,0}$ mode and coupling on the top port to the $WGH_{9,0,0}$ mode was measured as a function of temperature between 270 K and 350 K (see Fig. 11). From a comparison with the unloaded Q-factor data for these modes [16], within experimental error, the WGE-mode data has the same power law dependence for coupling (β) and Q. Therefore, the ratio of β/Q is constant leading to the conclusion that the observed change in coupling is entirely due to the changes in the internal losses in the resonator. However, for the WGH-mode data this was not observed to be the case. The coupling has a stronger dependence than the Q-factor and hence, the ratio of β/Q is not constant. A possible explanation for this is that since the side probes lock the position of the field pattern, the top coupling probe is not locked exactly to the maxima of the field energy and as the resonator is cooled the geometry changes slightly and the field pattern rotates slightly during cooling.

12

VII. CONCLUSION

The quality factor of 4 different sapphire resonators have been measured and compared near room temperature. We have developed simple resonator design rules based on these measurements. We have also explored optimal coupling architectures and it was found that straight electric-field antenna probes resulted in lower microwave losses than when magnetic-field loop probes were used to couple to some mode families. We also examined in detail which particular features determine the azimuthal location of the field maxima in the mode pattern. We noted that in some circumstances it was the coupling probes that determined this location although when we optimally coupled to the mode we discovered that it was some cylindrical asymmetry in the resonator itself that determined the field pattern. These explorations have allowed us to determine the optimum Q-factor for a microwave sapphire resonator at room temperature.

VIII. ACKNOWLEDGMENTS

[1] E. N. Ivanov, M. E. Tobar, and R. A. Woode, "Applications of interferometric signal processing to phase noise reduction in microwave oscillators," IEEE Trans. on Microw. Theory Tech., vol. 46, pp. 1537–1545, 1998.

[2] E.N. Ivanov and M.E. Tobar, "Low phase noise microwave oscillators with interferometic signal processing," IEEE Trans. on Microw. Theory Tech., vol. 54, no. 8, pp. 3284-3294, 2006.

[3] M.E. Tobar, E.N. Ivanov, R.A. Woode, J.H. Searls and A.G. Mann, "Low noise 9 GHz sapphire resonator-oscillator with thermoelectric temperature stabilisation at 300 Kelvin," IEEE Microwave and Guided Wave Letters, vol. 5, no. 4, pp. 108–110, 1995.

[4] R.J. Besson, M. Mourey, S. Galliou, F. Marionnet, F. Gonzalez, P. Guillemot, R. Tjoelker, W. Diener, and A. Kirk, "10 MHz hyperstable quartz oscillators performances," Joint Meeting European Frequency and Time Forum-IEEE International Frequency Control Symposium, vol. 1, pp. 326–330, 1999.

[5] J.G. Hartnett, N.R. Nand and C. Lu, "Ultra-low-phase-noise cryocooled microwave dielectric-sapphire-resonator oscillators," Appl. Phys. Lett., vol. 100, 183501, 2012.

[6] N.R. Nand, J.G. Hartnett, E.N. Ivanov, G. Santarelli, "Ultra-stable very-low-phase-noise signal source for Very Long Baseline Interferometry using a cryocooled sapphire oscillator," IEEE Trans on Microw. Theory Tech., vol. 59, no. 11, 2978–2986, 2011.

[7] E.N. Ivanov, D.G. Blair, V.I. Kalinichev, "Approximate approach to the design of shielded dielectric disk resonators with whispering-gallery modes," IEEE Trans on Microw. Theory Tech., vol. 41 , no. 4, pp. 632–638, 1993.

[8] O. Di Monaco, W. Daniau, I. Lajoie, Y. Gruson, M. Chaubet, V. Giordano, "Mode selection for a whispering gallery mode resonator," Electronics Letters, vol. 32, no. 7, pp. 669–670, 1996.

[9] G.J. Dick and J. Saunders, "Measurement and analysis of a microwave oscillator stabilized by a sapphire dielectric ring resonator for ultra low noise," IEEE Trans. Ultrason. Ferroelec. Freq. Contr., vol. 37, no.5, pp. 339–346, 1990.

[10] G.J. Dick and D.G. Santiago, "Microwave frequency discriminator with a cryogenic sapphire resonator for ultra-low phase noise," in Proc. of 6th European Frequency and Time Forum, Noordwijk, Nederlands, March 1992, pp. 35–39, 1992.

[11] J.G. Hartnett, M.E. Tobar, "Frequency-temperature compensation techniques for high-Q microwave resonators," in Frequency Measurement and Control: Advanced Techniques and Future Trends, Editor: A.N. Luiten, Springer-Verlag Topics in Applied Physics, vol. 79, pp. 67–91, 2001.

[12] A.A. Barannik, S.A. Bunyaev, N.T. Cherpak, Y.V. Prokopenko, A.A. Kharchenko, S.A. Vitusevich, "Whispering Gallery Mode Hemisphere Dielectric Resonators With Impedance Plane," IEEE Trans. on Microw. Theory Tech., vol. 58, no. 10, pp. 2682–2691, 2010.

[13] M.E. Tobar, A.J. Giles, S. Edwards, and J.H. Searls, "High-Q TE stabilized sapphire microwave resonators for low noise applications," IEEE Transactions on Ultrasonics, Ferroelectrics and Frequency Control, vol. 41, pp. 391–396, 1994.

[14] J. Krupka, K. Derzakowski, A. Abramowicz, M.E. Tobar, R.G. Geyer, "Use of whispering-gallery modes for complex permittivity determinations of ultra-low-loss dielectric materials," IEEE Trans. on Microw. Theory Tech., vol. 47, no. 6, pp. 752–759, 1999.

[15] J. Krupka, K. Derzakowski, M.E. Tobar, J.G. Hartnett, R.G. Geyer, "Complex permittivity

of some ultralow loss dielectric crystals at cryogenic temperatures," Meas. Sci. Technol., vol. 10, no. 4, 387–392, 1999.

[16] J.G. Hartnett, M.E. Tobar, E.N. Ivanov, and J. Krupka, "Room Temperature Measurement of the Anisotropic Loss Tangent of Sapphire Using the Whispering Gallery Mode Technique," IEEE Trans on Ultrasonics, Ferroelectrics and Frequency Control, vol. 53, no. 1, 34–38, 2006.

[17] A.N. Luiten, A.G. Mann, and D.G. Blair, "High resolution measurement of the temperature-dependence of the Q, coupling and resonant frequency of a microwave resonator," IOP Meas. Sci. Technol., vol. 7, pp. 949–953, 1996.

[18] M.E. Tobar, E.N. Ivanov, J.G. Hartnett, D. Cros, P. Bilski, "Cryogenic dual-mode resonator for a fly-wheel oscillator for a caesium frequency standard," IEEE Trans. UFFC, vol. 49, no. 10, pp. 1349–1355, 2002.

[19] A.N. Luiten, "Sapphire Secondary Frequency Standards," PhD Thesis, the University of Western Australia, 1995.